

Correlation Between Hydrochemical Component of Surface Water and Groundwater in Nida Valley, Poland

Cong Ngoc Phan^{1,2*}, Andrzej Strużyński¹, Tomasz Kowalik¹

¹ Faculty of Environmental Engineering and Land Surveying, University of Agriculture in Krakow, al. Mickiewicza 24/28, 30-059, Kraków, Poland

² Institute of Chemistry, Biology and Environment, Vinh University, 182 Le Duan St, Vinh City, Nghe An Province, Vietnam

* Corresponding author's e-mail: phancongngoc1402@gmail.com

ABSTRACT

The Nida valley study area underwent examination to investigate the hydrochemical components and the correlation between groundwater (GW) and surface water (SW). Over a 12-month period from November 2021 to October 2022, 9 monitoring points were established, consisting of 7 GW points and 2 SW points, with a monitoring frequency of once per month. The research findings indicate that the hydrochemical components and direction of GW flow in the study area can be classified into 3 distinct regions. The chemical composition is complex in areas near the Nida River, stable in the region near the Smuga Umianowicka branch, and different in other areas. It was observed that the SW in the Nida River and Smuga Umianowicka branch exhibits a relatively uncomplicated chemical composition due to minimal human impact in the natural area. However, dissimilarities between them were also identified and explained by the flow regulation of the dam built on the branch within the study area. The application of the Shapiro-Wilk test ($\alpha = 0.05$) and Kruskal-Wallis test ($\alpha = 0.05$) revealed statistically significant differences among the recorded hydrochemical component values throughout the measurement period. Furthermore, Pearson's correlation coefficient analysis ($\alpha = 0.001$) indicated correlations between the hydrochemical components of SW and GW in the riparian area and strong correlations among GW samples. Principal Component Analysis (PCA) identified significant dissimilarity and similarity between GW and SW samples based on their characteristics.

Keywords: correlation, groundwater, surface water, Nida valley, hydrochemical component.

INTRODUCTION

Surface water (SW) and groundwater (GW) are traditionally regarded as distinct components in nature and are typically studied independently. However, there exists a crucial transition zone between the two, where various processes influence the transportation, decomposition, and absorption of substances. In this area might also contain a proportion of SW due to infiltration, leading to unique characteristics of the water body. It was considered as essential zone for the metabolic processes of stream biota and stream metabolism (Hynes, 1983; Brunke and Gonser, 1997).

Interactions between GW and SW occur through two primary mechanisms: GW flows into

streams, and stream water infiltrates into the GW. The direction of this flow exchange depends on the hydraulic head, where gaining reaches possess a higher GW table elevation than the stream stage, while losing reaches have a lower GW table elevation (Savant et al., 1987; Thibodeaux and Boyle, 1987; Hutchinson and Webster, 1998). These exchanges of water between SW and GW can significantly impact the water quality of both systems (Phan et al., 2023).

Variations in the rate and occurrence of specific processes can have a profound impact on the composition and quantity of dissolved material carried by stream water. Subsurface water exchange plays a crucial role in determining the nature of substances and expedites their

transformation as water flows through the system. When there is substantial water exchange in sedimentary layers, the amount of time water spends in a particular reach and its interaction with subsurface sediments can cause significant alterations to the material being transported from the catchment to the receiving area. Moreover, when stream water comes into contact with mineral surfaces, anaerobic zones, or experiences intrusion from GW, unexpected changes in its composition can occur (Findlay, 1995; Kowalik et al., 2015; Bogdał et al., 2016). High metabolic rates in most sediments lead to nutrient regeneration and the reintroduction of mineral nutrients to the stream (Valett et al., 1990; Hendricks and White, 1991). Consequently, the water flowing back into the stream may carry elevated levels of inorganic nitrogen (N) and phosphorus (P), which could potentially result in increased water composition at these discharge sites (Valett et al., 1994). These factors collectively contribute to shaping the characteristics and quality of water as it moves through the stream system, highlighting the intricate relationship between subsurface processes and the overall chemical makeup of stream water.

To conserve water resources effectively, it becomes important to comprehend and quantify the interaction between GW and SW. In his work from 2000, Woessner emphasizes the significance for hydrogeologists to broaden their perspective and explore water exchange within the framework of riparian management, employing various methods. Various approaches have been employed to analyze the interaction between SW and GW (Lee, 1977; Kalbus et al., 2006; Wałęga et al., 2016). Early methods primarily centered on measurement techniques (Lee and Cherry, 1979; Woessner and Sullivan, 1984; Isiorho and Meyer, 1999), hydraulic gradient methods (Freeze and Cherry, 1979; Baxter et al., 2003), and numerical simulations (Frei et al., 2009; Boano et al., 2010; Jin et al., 2010). Environmental monitoring include the use of stable isotopes (deuterium and oxygen) (Négre et al., 2003; Xu et al., 2017), radioactive isotopes like strontium (Hakam et al., 2001), radium (Cook et al., 2003), and radon (Unland et al., 2013; Oyarzún et al., 2014) and hydrochemical analysis (Wang et al., 2013; Martinez et al., 2015). These methods have proven effective for both small-scale studies (Jones et al., 2008; Guay et al., 2013) and regional studies (Jutebring Sterte et al., 2018a; Wang et al., 2018). The integration of numerical simulation alongside field

measurement techniques, isotopic, and hydrochemistry analysis has proven to be highly effective in yielding valuable insights.

In this study, method for measuring hydrochemical analysis was utilised to analyze the correlation between SW and GW. The hydrochemical component can be determined by gathering GW samples in monitoring wells. Monitoring wells should be installed in close proximity along transects through the contaminant plume to obtain trustworthy results. The use of multi-layered monitoring wells provides a 3D of representation of hydrochemical component (Borden et al., 1997; Pitkin et al., 1999; Conant et al., 2004). An extensive network of monitoring wells can furnish precise data regarding the distribution of components. The hydrochemical component in SW can be determined by analyzing water samples from various sources, such as grab or bottle samples. However, this method has limitations as it only provides a momentary representation of component levels at the time of sampling, and a significant amount of water sample is required when the contaminants are present in trace amounts (Vrana et al., 2005). To overcome these challenges, automated sampling systems can be utilised for continuous monitoring over a long period.

The aim of this study is to investigate the hydrochemical composition of SW and GW, as well as to establish correlations between them. Subsequently, we intend to discern the direction of subterranean water flow and explore the interactions between GW and SW within the designated study area.

MATERIALS AND METHODS

Study area

The interested subject is situated in the Nida Valley, which is located in Poland, Europe. This river valley is characterized by vast plains, grasslands, and inundated forests, with a typical soil structure consisting of sand covered by a thin layer of mud. The formation of the valley is attributed to the Nida River's course near the town of Pińczów. In this valley there are three branches. The two active were the Nida River itself and the Smuga Umianowicka branch while the Stara Nida branch was dry during measurement session. The specific measurement section lies inside the Nadnidziański Landscape Park, forming

a crucial segment of a significant wildlife area (Strużyński et al., 2015). The investigation site encompasses the region between the Nida River and the Smuga branch, situated in the Pińczów district (Figure 1). The Nida Valley floodplain experiences regular flooding during the spring season and occasional flooding during summer, with inundation persisting for a duration of 2 to 5 months each year. Notably, the floodplain is widest, ranging from 0.3 to 5.0 kilometers, near the location of Umianowice. This floodplain plays a crucial role as a natural storage area for water, effectively mitigating the risk of riverine flooding (Borek and Drymajło, 2019). As highlighted by Łajczak (2004), this natural function of the floodplain helps to regulate water levels and prevent excessive flooding incidents. The course of the Nida River has been modified on numerous occasions as a result of flood control measures. Some sections of the river have had their flow artificially shortened. From the 1960s to the early 20th century, the flow of the Nida was regulated, resulting in a shortened river. However, the rivers further downstream still maintain their natural flow. As a result of these changes, the Nida Valley has lost its natural ecological function and is nearly drained, with remnants of former marshes and water remaining. This is where you can observe

both the beneficial and detrimental consequences of past flood control measures (Żelazo, 1993; Łajczak, 2004).

Environmental monitoring method

Choice of sampling locations

Nine sampling points were carefully chosen in the Nadnidziański Landscape Park. Among these points, seven were designated as GW (from GW1 to GW7) and were used to collect GW samples. These sampling locations consist of 2-meter-deep wells with a 10-centimeter diameter, strategically drilled at cross-sections every 150–200 meters. Stabilized with plastic pipes, these wells serve as sampling points. Additionally, two sampling points, identified as SW, were located in the stream, with SW1 situated at the Nida River and SW2 at the Smuga Umianowicka branch. The sampling region was thoughtfully settled along the Nida Valley, starting from the regulated channel of the Nida, extending through the Smuga Umianowicka branch. The distance of approximately 1365 meters from the river's primary channel (Figure 1).

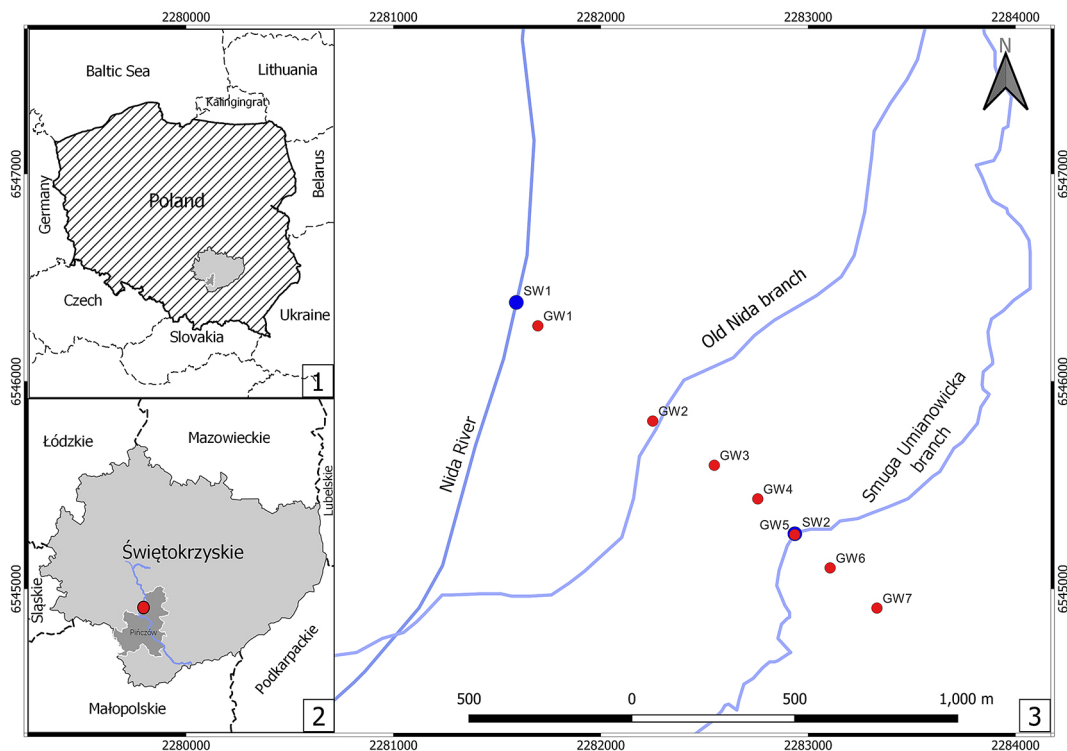


Fig. 1. Map of study area and sampling sites in the Nida valley; source: own elaboration Explanation: Red points: groundwater collected locations. Blue points: water surface collected locations.

Sample collection

The sampling period extended for 12 months, commencing in October 2021 and concluding in November 2022, with a monthly sampling frequency. A total of 108 water samples were gathered from 9 distinct sampling locations. The sample collection device used is a vertical tube with a check valve. The samples are stored in 300 cm³ bottles and promptly carried to the laboratory. They are stored in a refrigerator at 4°C to maintain their integrity.

Physical parameters

During the sample collection, physical parameters such as total dissolved solids (TDS) was measured on-site using a dissolved substances meter (TDS-3).

Laboratory experiments

The experiments were conducted following the standard methods as recommended by the American Public Health Association (APHA, 1998) and the Environmental Protection Agency (EPA 1983). The hydrochemical parameters include total nitrogen (TN), total phosphorus (TP), chloride (Cl⁻), sulphate (SO₄²⁻), manganese (Mn²⁺), iron (Fe^{2+,3+}), zinc (Zn²⁺), lead (Pb²⁺). Total nitrogen (TN) and total phosphorus (TP) were quantified using the flow analysis method employing the FiaCompact MLE flow analyzer equipped with a mineralizer. Additionally, chloride (Cl⁻) was determined utilizing the flow analysis method employing the FiaSTAR flow analyzer. Sulphate (SO₄²⁻) was determined using the turbidimetric method. The concentrations of iron (Fe^{2+,3+}), manganese (Mn²⁺), and zinc (Zn²⁺) were measured utilizing the atomic absorption spectrometry method (AAS) with a Unicam Solar atomic absorption spectrophotometer at respective wavelengths of 248.3 nm, 249.5 nm, and 213.9 nm. Lead (Pb) was determined through the colorimetric method by the EcaFlow colorimetric analyzer. The limits of detection (LOD) and limits of quantitation (LOQ) for the parameters are shown in Table 1.

Data and statistical analysis

The Shapiro–Wilk test (with a significance level of $\alpha = 0.05$) was employed to assess whether the variables adhered to a normal distribution.

To evaluate the significance of differences between samples collected at different times, a non-parametric analysis (Kruskal–Wallis test) with a significance level of $\alpha = 0.05$ was carried out. Besides, the correlation between the hydrochemical parameters of groundwater and surface water was determined by computing Pearson’s correlation coefficients (r) and creating a correlation matrix. The significance of the coefficients was determined by examining the r -value with a significance level set at 0.001. Moreover, Principal Component Analysis (PCA) was applied to establish connections between the collected samples throughout the study period and determine the hydrochemical parameters influencing each sample. The analysis was conducted using R version 4.1.2, which is open-source software distributed under the GNU license.

RESULTS AND DISCUSSION

The hydrochemical composition of water

The Shapiro-Wilk test and Kruskal-Wallis test were performed, and the outcomes are presented in Table 2. The p -values obtained from the Shapiro-Wilk test were below 0.05 for all observed parameters, indicating that the variables adhered to a normal distribution. Moreover, the results of the Kruskal-Wallis test also revealed p -values below 0.05 for all observed parameters, suggesting statistically significant differences among the recorded values of the parameters throughout the measurement period.

The ionic composition in water reflects the interaction between rock and water during the flow path (Edmunds et al., 2003; Möller et al.,

Table 1. Limit of detection (LOD) and limit of quantitation (LOQ) for the parameters

Parameter	Measurement unit	LOD	LOQ
TN	mg·dm ⁻³	0.05	0.05
TP	mg·dm ⁻³	0.005	0.01
Pb ²⁺	µg·dm ⁻³	0.5	1.00
Cl ⁻	mg·dm ⁻³	0.1	1.00
Fe ^{2+,3+}	mg·dm ⁻³	0.027	0.0743
Mn ²⁺	mg·dm ⁻³	0.009	0.027
Zn ²⁺	mg·dm ⁻³	0.0065	0.0198
SO ₄ ²⁻	mg·dm ⁻³	0.01	1

Note: Based on laboratory equipment specifications.

Table 2. The results of Shapiro-Wilk test and Kruskal-Wallis test for each observation parameter

Observation parameter	Shapiro-Wilk test		Kruskal-Wallis test		
	W	p-value	Chi-squared	df	p-value
TN	0.589	1.008e-13	27.560	6	1.137e-04
TP	0.468	1.279e-15	15.545	6	1.642e-02
Cl ⁻	0.858	2.612e-07	31.203	6	2.319e-05
SO ₄ ²⁻	0.869	6.619e-07	41.304	6	2.523e-07
Mn ²⁺	0.863	4.052e-07	21.511	6	1.484e-03
Fe ^{2+,3+}	0.649	1.269e-12	31.588	6	1.957e-05
Zn ²⁺	0.481	1.975e-15	23.421	6	6.672e-04
Pb ²⁺	0.593	1.229e-13	24.504	6	4.218e-04

2007). Figure 2 presents the observed data of water chemistry. In the study area, the GW displays a clear hydrochemical zonation as it flows from the riparian zone to the Nida River, reflecting hydrodynamic processes influenced by the interaction between SW and GW. Specifically, GW1 in the riparian zone of the Nida valley is characterized by the presence of TN•Cl•SO₄²⁻•Mn²⁺•Fe^{2+,3+}•Zn²⁺•Pb²⁺, with a TDS ranging from 149 to 651 mg.dm⁻³. In the GW2 zone, the GW chemistry is characterized by Cl•SO₄²⁻•Mn²⁺•Fe^{2+,3+}•Zn²⁺•Pb²⁺, with TDS values ranging from 159 to 643 mg.dm⁻³. Moving further along the flow path, the hydrochemical types of GW3 zone are mostly Cl•SO₄²⁻•Mn²⁺•Fe^{2+,3+}•Zn²⁺•Pb²⁺, and the TDS ranges from 328 to 627 mg.dm⁻³. The hydrochemical types of GW4 zone are mostly Cl•SO₄²⁻•Mn²⁺•Fe^{2+,3+}•Zn²⁺, with the TDS ranging from 113 to 458 mg.dm⁻³. Similarly, the hydrochemical types of GW5 zone are mostly Cl•SO₄²⁻•Mn²⁺•Fe^{2+,3+}, with the TDS ranging from 338 to 694 mg.dm⁻³. The hydrochemical types of GW6 zone are mostly Cl•SO₄²⁻•Mn²⁺•Fe^{2+,3+}, with the TDS ranging from 425 to 711 mg.dm⁻³. Finally, in the GW7 zone, the hydrochemical types of GW are mostly Cl•Fe^{2+,3+}•Zn²⁺, with the TDS ranging from 74 to 158 mg.dm⁻³.

The hydrochemistry of GW is primarily influenced by dissolution, evaporation, and filtration (Qian and Li, 2011; Jing et al., 2014). It is predominantly affected by precipitation and leaching processes (Jing et al., 2014). The resemblance in chemical types among the GW observation points suggests their interconnectedness through underground flows (Zhu et al., 2019). In this study, the water's chemical types exhibit greater complexity in locations near the Nida River (GW1) and relatively simpler types in more distant locations (GW2, GW3, GW4). Besides, the TDS value decreases gradually from GW1 to GW4. This

pattern indicates a tendency for GW to flow from the riparian area towards the Nida River, specifically from location GW4 to GW1. However, the similarity in chemical types and TDS value observed between GW5 and GW6 indicates a close association between these two sites. Conversely, at GW7, the water's chemical types and the lowest TDS value are distinct from other locations, implying a difference in its characteristics and direction of underground flow from GW7 to GW6.

Typically, the composition of river water is more intricate compared to GW, primarily due to the influence of human activities as it passes through residential areas. However, in this study, the Nida River's flow characteristics through a natural area have resulted in minimal impact from human activities. As a result, the composition of river water in this region is relatively uncomplicated. The dominant chemical types observed in SW1 of the Nida River are TN•Cl, with a TDS ranging from approximately 129 to 268 mg.dm⁻³. On the other hand, SW2 in the Smuga Umianowicka branch is mainly composed of Cl•SO₄²⁻, with TDS levels ranging from approximately 261 to 326 mg.dm⁻³.

The correlation between the hydrochemical properties of groundwater and river water

Pearson's correlation coefficient analysis

The correlation coefficients (r) for all data points are presented in the correlation matrix (Figure 3), accompanied by their corresponding significance levels (p-values). In all cases, a positive correlation was observed, with correlation coefficients (r) greater than 0.5 and p-values less than 0.001.

Strong positive correlations were found between GW1 and GW3 (r = 0.9), GW6 (r = 0.93), GW5 (r = 0.86), GW7 (r = 0.9), and GW2

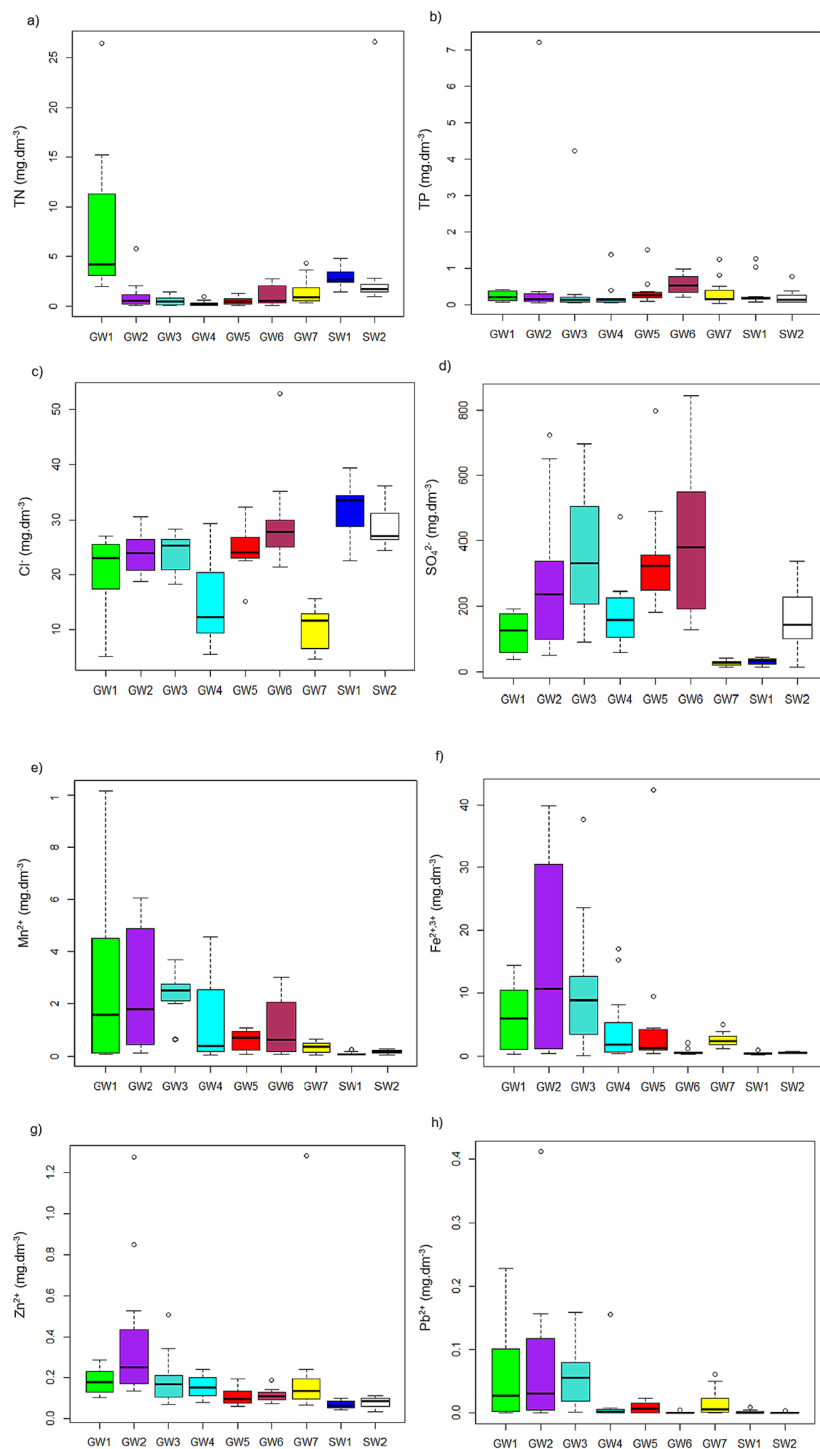


Fig. 2. The hydro-chemical values of water at the observation points: a) total nitrogen (TN), b) total phosphorus (TP), c) chloride (Cl⁻), d) sulphate (SO₄²⁻); e) manganese (Mn²⁺), f) iron (Fe^{2+,3+}), g) zinc (Zn²⁺), h) lead (Pb²⁺); Explanation: In the rectangles, average values are displayed, along with standard deviation limits. The minimum and maximum values are indicated by the whiskers, which represent the lowest and highest values. Any outliers are represented by small circles.

($r = 0.8$). Additionally, significant positive correlations were observed between GW3 and GW6 ($r = 0.98$), GW5 ($r = 0.85$), GW7 ($r = 0.85$), and GW2 ($r = 0.85$). Furthermore, there were significant positive correlations between GW6 and

GW5 ($r = 0.83$), GW7 ($r = 0.84$), GW2 ($r = 0.86$), as well as between GW5 and GW7 ($r = 0.86$), and GW7 and SW1 ($r = 0.85$).

The results of this study indicate a correlation between the hydrochemical composition of

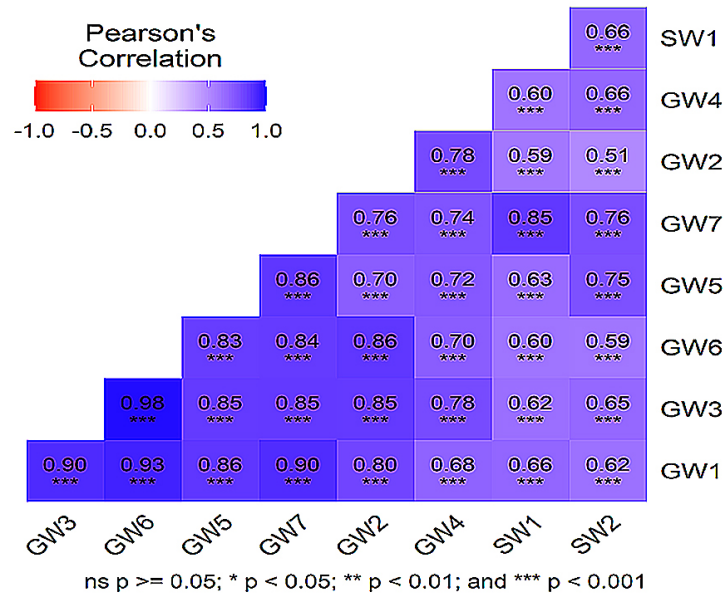


Fig. 3. Correlation matrix of the hydrochemical properties at the observed points

SW and GW in the riparian area. Particularly, there were strong correlations between GW1 and GW2, GW3, GW5, GW6, and GW7. Additionally, GW3 showed correlations with GW5, GW6, GW7, and GW2. Similarly, GW6 exhibited correlations with GW5, GW7, and GW2. Moreover, GW5 displayed a correlation with GW7, and GW7 showed a correlation with SW1.

The correlations between the hydrochemical composition of SW and GW in the studied area, characterized by a high concentration of dissolved minerals, can be attributed to rock weathering processes (Costello et al., 1984; Nowobilska-Luberda, 2018). The hydrochemical composition of GW in the riparian area shows a strong correlation, indicating the exchange of GW between observation points within the study area. The research conducted by Phan et al. (2023) on the groundwater in Nida valley revealed significant concentrations of Mn^{2+} and $Fe^{2+,3+}$. The physicochemical analysis indicated that these elements are present at notably high levels. Additionally, the study demonstrated seasonal variations in groundwater properties, with the content of various compounds being particularly elevated during summer and lower during other seasons. On the other hand, the correlation between the hydrochemical composition of SW and GW is weaker, which can be attributed to the dilution or addition of compounds in the stream as it passes through various regions, resulting in heterogeneous changes in the hydrochemical properties of SW (Demaku and Bajraktari, 2019).

Furthermore, a weak correlation is observed between the hydrochemical composition of SW in the Nida River (SW1) and the Smuga Umianowicka branch (SW2). This lack of correlation can be attributed to the disruption in the flow at the Smuga Umianowicka branch caused by the construction of a dam aimed at regulating its flow (Cel et al., 2017; Phan et al., 2023). Wojak et al. (2023), in their investigation of hydraulic properties through measurements and simulations of a segment of the Nida River, demonstrated the existence of unequal relationships between the flow of water and the river bed. Variations in river discharge not only affect the magnitude of the flow processes, but also water component.

Principal Component Analysis (PCA)

The results of PCA explained four factors, accounting for a cumulative explanation of 74.7% of the total variance and visualized in the PCA-biplot as follows: 30.8% for Dimension 1 (Dim1) and 17.5% for Dimension 2 (Dim2) in Figure 4a, and 14.3% for Dimension 3 (Dim3) and 12.1% for Dimension 4 (Dim4) in Figure 4b.

Dim1 exhibited positive loading for Mn^{2+} , Zn^{2+} , SO_4^{2-} , Cl^- , TN, Pb^{2+} , $Fe^{2+,3+}$, and negative loading for TP. Notably, among these variables, Mn^{2+} and Pb^{2+} exhibited the strongest positive loading, while TP displayed the strongest negative loading when compared to the other variables. Therefore, as the levels of Mn^{2+} and Pb^{2+} increase, it is likely that the other parameters will also increase. Conversely, when TP decreases,

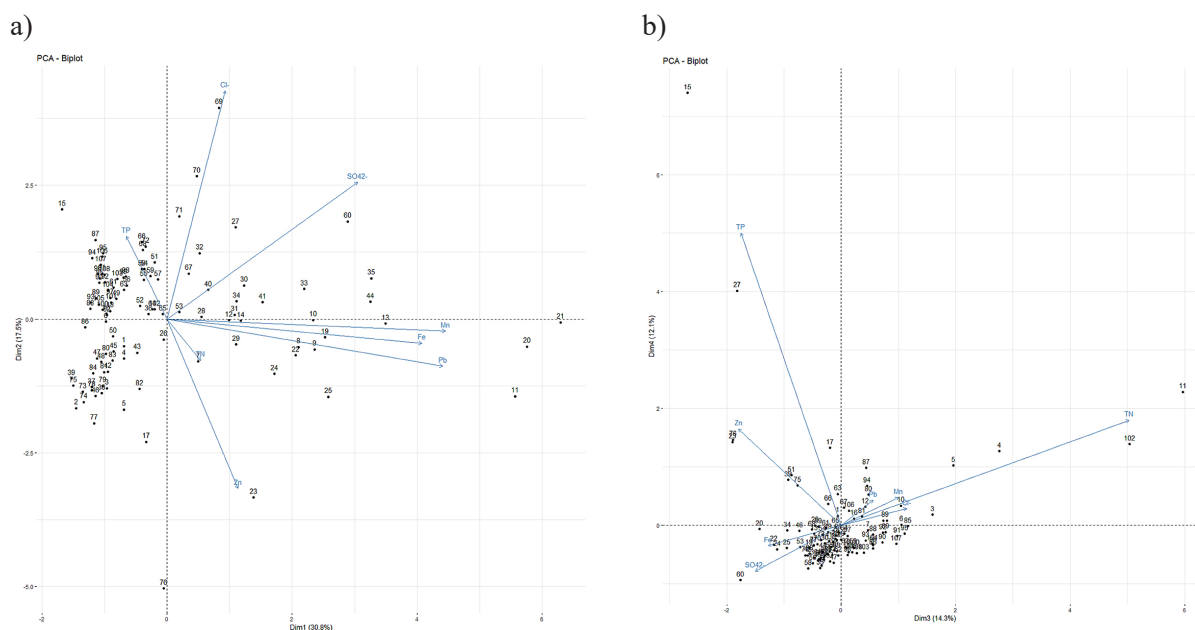


Fig. 4. Biplot – resulting from the principal component analysis: a) Dim1, Dim2; b) Dim3, Dim4

it can lead to an increase in the other variables. Furthermore, Dim1 revealed a pronounced dissimilarity between sample of September 2022 at GW1 (point No. 11), May 2022 at GW2 (point No. 20) and June 2022 at GW2 (point No. 21) when compared to the other samples. Conversely, it showed a strong similarity among the samples taken in September 2022 at GW1 (point No. 11), May 2022 at GW2 (point No. 20), and June 2022 at GW2 (point No. 21). They are characterized by high Mn^{2+} , $Fe^{2+,3+}$, Pb^{2+} content. Dim1 also shows a clustering concentration of surface water samples at SW1 and SW2 (numbers 85 to 96 for SW1 and from 97 to 108 for SW2) and they are characterized by high phosphorus content.

Dim2 demonstrated positive loading with SO_4^{2-} , Cl^- , TP and negative loading with Mn^{2+} , Pb^{2+} , $Fe^{2+,3+}$, Zn^{2+} and TN. The Cl^- , SO_4^{2-} variations showed the strongest positive loading and Zn^{2+} variation showed the weakest positive loading. Dim2 also performed a strong dissimilarity was obtained between sample of July 2022 at GW6 (point No. 69) with sample of September 2022 at GW2 (point No. 23) and February 2022 at GW7 (point No. 76) due to high content of Cl^- at GW6 and Zn^{2+} at GW2 and GW7.

Dim3 described negative loading with TP, Zn^{2+} , $Fe^{2+,3+}$, SO_4^{2-} , and positive loading with TN, Mn^{2+} , Pb^{2+} , and Cl^- . The most substantial positive loading was observed in the case of TN, indicating that an increase in TN would likely result in an increase in the other parameters. Dim3 also displayed a pronounced dissimilarity between January, February,

March 2022 at GW1 (point No. 3, 4, 5) and September 2022 at GW1 (point No. 11), April 2022 at SW2 (point No. 102) with others. Therein, they are characterised by high content of TN.

Dim4 showed negative loading with Fe, SO_4^{2-} , and positive loading with TP, TN, Pb^{2+} , Zn^{2+} , Mn^{2+} , and Cl^- . The most prominent positive loading was associated with TP, indicating that an increase in TP would likely lead to an increase in the other parameters. Dim4 exhibited a significant dissimilarity between sample of January 2022 at GW2 (point No. 15) and January 2022 at GW3 (point No. 27) with others. Therein, these samples are characterized by a high content of TP. Besides, Dim4 also indicated high similarity of the remaining samples.

CONCLUSIONS

This study used the environmental monitoring method to observe the hydrochemical composition and the correlation between hydrochemical component of GW and SW in the Nida valley, Poland. Research results indicate that the chemical complexity of GW is higher near the Nida River (GW1) and simpler in more distant locations (GW2, GW3, GW4). TDS value gradually decreases from GW1 to GW4, suggesting a flow tendency from GW4 to GW1. GW5 and GW6 show similarity in chemical types and TDS value, indicating a close association between these sites. In contrast, GW7 exhibits distinct

chemical types and the lowest TDS value, implying different characteristics and underground flow direction from GW7 to GW6. SW in the Nida River and Smuga Umianowicka branch have relatively uncomplicated chemical compositions due to minimal impact from human activities in the natural area.

The Shapiro-Wilk test ($\alpha = 0.05$) and Kruskal-Wallis test ($\alpha = 0.05$) revealed statistically significant differences among the recorded parameter values throughout the measurement period. Pearson's correlation coefficient analysis ($\alpha = 0.001$) indicated strong correlations between the hydrochemical composition of SW and GW in the riparian area. Specifically, GW1 correlated strongly with GW2, GW3, GW5, GW6, and GW7. GW3 showed correlations with GW6, GW5, GW7, and GW2. GW6 exhibited correlations with GW5, GW7, and GW2. Additionally, GW5 displayed a correlation with GW7, and GW7 showed a correlation with SW1.

Principal Component Analysis (PCA) found strong dissimilarity observed between samples from September 2022 at GW1 (point No. 11), May 2022 at GW2 (point No. 20), and June 2022 at GW2 (point No. 21) compared to other samples. These three samples show high Mn^{2+} , $Fe^{2+,3+}$, and Pb^{2+} content, indicating a close similarity between them. SW samples at SW1 (points No. 85 to 96) and SW2 (points No. 97 to 108) cluster together, showing high phosphorus content. Sample from July 2022 at GW6 (point No. 69) differs significantly from samples in September 2022 at GW2 (point No. 23) and February 2022 at GW7 (point No. 76) due to high Cl⁻ content at GW6 and Zn^{2+} content at GW2 and GW7. January, February, and March 2022 samples at GW1 (points No. 3, 4, 5) and September 2022 at GW1 (point No. 11), and April 2022 at SW2 (point No. 102) show strong dissimilarity from others, characterized by high TN content. January 2022 sample at GW2 (point No. 15) and January 2022 at GW3 (point No. 27) differ significantly from others due to high TP content. The remaining samples exhibit high similarity.

The obtained results are both consistent and dependable. This study is currently ongoing, and over the next two years, additional data will be collected and added. These findings can serve as valuable reference data for future water studies in the Nida Valley.

REFERENCES

1. APHA 1998. Standard methods for the examination of water and wastewater. 20th ed. Washington, DC. American Public Health Association. ISBN 0875532357, 1325.
2. Baxter, C., Hauer, F.R., Woessner, W.W., 2003. Measuring groundwater–stream water exchange: New techniques for installing minipiezometers and estimating hydraulic conductivity. *Transactions of the American Fisheries Society* 132, 493–502. [https://doi.org/10.1577/1548-8659\(2003\)132<0493:MGWENT>2.0.CO;2](https://doi.org/10.1577/1548-8659(2003)132<0493:MGWENT>2.0.CO;2)
3. Boano, F., Revelli, R., Ridolfi, L., 2010. Effect of streamflow stochasticity on bedform-driven hyporheic exchange. *Advances in Water Resources* 33, 1367–1374. <https://doi.org/10.1016/j.advwatres.2010.03.005>
4. Bogdał, A., Kowalik, T., Ostrowski, K., Skowron, P., 2016. Seasonal variability of physicochemical parameters of water quality on length of Uszwica river. *J. Ecol. Eng.*; 17(1), 161–170; <https://doi.org/10.12911/22998993/61206>
5. Borden, R.C., Daniel, R.A., LeBrun, L.E., Davis, C.W., 1997. Intrinsic biodegradation of MTBE and BTEX in a gasoline-contaminated aquifer. *Water Resour. Res.* 33, 1105–1115. <https://doi.org/10.1029/97WR00014>
6. Borek, Ł., Drymajło, K., 2019. The role and importance of irrigation system for increasing the water resources: the case of the Nida River valley. *ASP.FC* 18, 19–30. <https://doi.org/10.15576/ASP.FC/2019.18.3.19>
7. Brunke, M., Gonser, T., 1997. The ecological significance of exchange processes between rivers and groundwater. *Freshwater Biology* 37, 1–33. <https://doi.org/10.1046/j.1365-2427.1997.00143.x>
8. Cel, W., Kujawska, J., Wasąg, H., 2017. Impact of hydraulic fracturing on the quality of natural waters. *J. Ecol. Eng.* 18, 63–68. <https://doi.org/10.12911/22998993/67852>
9. Conant, B., Cherry, J.A., Gillham, R.W., 2004. A PCE groundwater plume discharging to a river: influence of the streambed and near-river zone on contaminant distributions. *Journal of Contaminant Hydrology* 73, 249–279. <https://doi.org/10.1016/j.jconhyd.2004.04.001>
10. Cook, P.G., Favreau, G., Dighton, J.C., Tickell, S., 2003. Determining natural groundwater influx to a tropical river using radon, chlorofluorocarbons and ionic environmental tracers. *Journal of Hydrology* 277, 74–88. [https://doi.org/10.1016/S0022-1694\(03\)00087-8](https://doi.org/10.1016/S0022-1694(03)00087-8)
11. Costello, M.J., McCarthy, T.K., O'Farrell, M.M., 1984. The stoneflies (Plecoptera) of the Corrib catchment area, Ireland. *Annls Limnol.* 20, 25–34. <https://doi.org/10.1051/limn/1984014>

12. Demaku, S., Bajraktari, N., 2019. Physicochemical Analysis of the Water Wells in the Area of Kosovo Energetic Corporation (Obiliq, Kosovo). *J. Ecol. Eng.* 20, 155–160. <https://doi.org/10.12911/22998993/109874>
13. Edmunds, W.M., Guendouz, A.H., Mamou, A., Moulla, A., Shand, P., Zouari, K., 2003. Groundwater evolution in the Continental Intercalaire aquifer of southern Algeria and Tunisia: trace element and isotopic indicators. *Applied Geochemistry* 18, 805–822. [https://doi.org/10.1016/S0883-2927\(02\)00189-0](https://doi.org/10.1016/S0883-2927(02)00189-0)
14. EPA 1983. Methods for chemical analysis of water and wastes. Washington, DC. United States Environmental Protection Agency, 491.
15. Findlay, S., 1995. Importance of surface-subsurface exchange in stream ecosystems: The hyporheic zone. *Limnol. Oceanogr.* 40, 159–164. <https://doi.org/10.4319/lo.1995.40.1.0159>
16. Freeze, R.A., Cherry, J.A., 1979. *Groundwater*. Prentice-Hall, Englewood Cliffs, N.J.
17. Frei, S., Fleckenstein, J.H., Kollet, S.J., Maxwell, R.M., 2009. Patterns and dynamics of river–aquifer exchange with variably-saturated flow using a fully-coupled model. *Journal of Hydrology* 375, 383–393. <https://doi.org/10.1016/j.jhydrol.2009.06.038>
18. Guay, C., Nastev, M., Paniconi, C., Sulis, M., 2013. Comparison of two modeling approaches for groundwater-surface water interactions: Comparison of two modeling approaches for gw-sw interactions. *Hydrol. Process.* 27, 2258–2270. <https://doi.org/10.1002/hyp.9323>
19. Hakam, O.K., Choukri, A., Moutia, Z., Chouak, A., Cherkaoui, R., Reyss, J.-L., Lferde, M., 2001. Uranium and radium in groundwater and surface water samples in Morocco. *Radiation Physics and Chemistry* 61, 653–654. [https://doi.org/10.1016/S0969-806X\(01\)00362-0](https://doi.org/10.1016/S0969-806X(01)00362-0)
20. Hendricks, S.P., White, D.S., 1991. Physicochemical Patterns within a Hyporheic Zone of a Northern Michigan River, with Comments on Surface Water Patterns. *Can. J. Fish. Aquat. Sci.* 48, 1645–1654. <https://doi.org/10.1139/f91-195>
21. Hutchinson, P.A., Webster, I.T., 1998. Solute Uptake in Aquatic Sediments due to Current-Obstacle Interactions. *J. Environ. Eng.* 124, 419–426. [https://doi.org/10.1061/\(ASCE\)0733-9372\(1998\)124:5\(419\)](https://doi.org/10.1061/(ASCE)0733-9372(1998)124:5(419))
22. Hynes, H.B.N., 1983. Groundwater and stream ecology. *Hydrobiologia* 100, 93–99. <https://doi.org/10.1007/BF00027424>
23. Isiorho, S.A., Meyer, J.H., 1999. The Effects of Bag Type and Meter Size on Seepage Meter Measurements. *Ground Water* 37, 411–413. <https://doi.org/10.1111/j.1745-6584.1999.tb01119.x>
24. Jin, G., Tang, H., Gibbes, B., Li, L., Barry, D.A., 2010. Transport of nonsorbing solutes in a streambed with periodic bedforms. *Advances in Water Resources* 33, 1402–1416. <https://doi.org/10.1016/j.advwatres.2010.09.003>
25. Jing, X., Yang, H., Cao, Y., Wang, W., 2014. Identification of indicators of groundwater quality formation process using a zoning model. *Journal of Hydrology* 514, 30–40. <https://doi.org/10.1016/j.jhydrol.2014.03.059>
26. Jones, J.P., Sudicky, E.A., McLaren, R.G., 2008. Application of a fully-integrated surface-subsurface flow model at the watershed-scale: A case study: Integrated surface-subsurface flow model. *Water Resour. Res.* 44. <https://doi.org/10.1029/2006WR005603>
27. Jutebring Sterte, E., Johansson, E., Sjöberg, Y., Huseby Karlsen, R., Laudon, H., 2018a. Groundwater-surface water interactions across scales in a boreal landscape investigated using a numerical modeling approach. *Journal of Hydrology* 560, 184–201. <https://doi.org/10.1016/j.jhydrol.2018.03.011>
28. Kalbus, E., Reinstorf, F., Schirmer, M., 2006. Measuring methods for groundwater – surface water interactions: a review. *Hydrol. Earth Syst. Sci.* 10, 873–887. <https://doi.org/10.5194/hess-10-873-2006>
29. Kowalik, T., Bogdał, A., Borek, Ł., Kogut, A., 2015. The effect of treated sewage outflow from a modernized sewage treatment plant on water quality of the Breń River. *J. Ecol. Eng.* 16, 96–102. <https://doi.org/10.12911/22998993/59355>
30. Lee, D.R., 1977. A device for measuring seepage flux in lakes and estuaries I. *Limnol. Oceanogr.* 22, 140–147. <https://doi.org/10.4319/lo.1977.22.1.0140>
31. Lee, D.R., Cherry, J.A., 1979. A Field Exercise on Groundwater Flow Using Seepage Meters and Mini-piezometers. *Journal of Geological Education* 27, 6–10. <https://doi.org/10.5408/0022-1368-27.1.6>
32. Łajczak A., 2004. Negative consequences of regulation of a meandering sandy river and proposals tending to diminish flood hazard. Case study of the Nida river, southern Poland. *Proceedings of the Ninth International Symposium on River Sedimentation*. Yichang, China. Beijing. IAHR, 1773–1783
33. Martinez, J.L., Raiber, M., Cox, M.E., 2015. Assessment of groundwater–surface water interaction using long-term hydrochemical data and isotope hydrology: Headwaters of the Condamine River, Southeast Queensland, Australia. *Science of The Total Environment* 536, 499–516. <https://doi.org/10.1016/j.scitotenv.2015.07.031>
34. Möller, P., Rosenthal, E., Geyer, S., Flexer, A., 2007. Chemical evolution of saline waters in the Jordan-Dead Sea transform and in adjoining areas. *Int J Earth Sci (Geol Rundsch)* 96, 541–566. <https://doi.org/10.1007/s00531-006-0111-9>
35. Négrel, Ph., Petelet-Giraud, E., Barbier, J., Gautier, E., 2003. Surface water–groundwater interactions in an alluvial plain: Chemical and isotopic systematics. *Journal of Hydrology* 277, 248–267. <https://doi.org/10.1016/j.jhydrol.2003.07.011>

- org/10.1016/S0022-1694(03)00125-2
36. Nowobilska-Luberda, A., 2018. Physicochemical and Bacteriological Status of Surface Waters and Groundwater in the Selected Catchment Area of the Dunajec River Basin. *J. Ecol. Eng.* 19, 162–169. <https://doi.org/10.12911/22998993/86329>
 37. Oyarzún, R., Barrera, F., Salazar, P., Maturana, H., Oyarzún, J., Aguirre, E., Alvarez, P., Jourde, H., Kretschmer, N., 2014. Multi-method assessment of connectivity between surface water and shallow groundwater: the case of Limarí River basin, north-central Chile. *Hydrogeol J* 22, 1857–1873. <https://doi.org/10.1007/s10040-014-1170-9>
 38. Phan, C.N., Strużyński, A., Kowalik, T., 2023. Monthly changes in physicochemical parameters of the groundwater in Nida valley, Poland (case study). *Journal of water and Land development* 220–234. <https://doi.org/10.24425/jwld.2023.143763>
 39. Pitkin, S.E., Cherry, J.A., Ingleton, R.A., Broholm, M., 1999. Field Demonstrations Using the Waterloo Ground Water Profiler. *Ground Water Monit. Remediat* 19, 122–131. <https://doi.org/10.1111/j.1745-6592.1999.tb00213.x>
 40. Qian, H., Li, P., 2011. Hydrochemical Characteristics of Groundwater in Yinchuan Plain and Their Control Factors. *Asian J. Chem.* 23, 2927–2938.
 41. Savant, S.A., Reible, D.D., Thibodeaux, L.J., 1987. Convective transport within stable river sediments. *Water Resour. Res.* 23, 1763–1768. <https://doi.org/10.1029/WR023i009p01763>
 42. Strużyński, A., Książek, L., Bartnik, W., Radecki-Pawlik, A., Plesiński, K., Florek, J., Wyrębek, M., Strutyński, M., 2015. Wetlands in River Valleys as an Effect of Fluvial Processes and Anthropoppression, in: Ignar, S., Grygoruk, M. (Eds.), *Wetlands and Water Framework Directive, GeoPlanet: Earth and Planetary Sciences*. Springer International Publishing, Cham, 69–90. https://doi.org/10.1007/978-3-319-13764-3_5
 43. Thibodeaux, L.J., Boyle, J.D., 1987. Bedform-generated convective transport in bottom sediment. *Nature* 325, 341–343. <https://doi.org/10.1038/325341a0>
 44. Unland, N.P., Cartwright, I., Andersen, M.S., Rau, G.C., Reed, J., Gilfedder, B.S., Atkinson, A.P., Hofmann, H., 2013. Investigating the spatio-temporal variability in groundwater and surface water interactions: a multi-technique approach. *Hydrol. Earth Syst. Sci.* 17, 3437–3453. <https://doi.org/10.5194/hess-17-3437-2013>
 45. Valett, H.M., Fisher, S.G., Stanley, E.H., 1990. Physical and Chemical Characteristics of the Hyporheic Zone of a Sonoran Desert Stream. *Journal of the North American Benthological Society* 9, 201–215. <https://doi.org/10.2307/1467584>
 46. Valett, H.M., Fisher, S.G., Grimm, N.B., Camill, P., 1994. Hydrologic exchange and ecological stability of a desert stream ecosystem, *Ecology*, 75, 548–560. <https://doi.org/10.2307/1939557>
 47. Vrana, B., Allan, I.J., Greenwood, R., Mills, G.A., Dominiak, E., Svensson, K., Knutsson, J., Morrison, G., 2005. Passive sampling techniques for monitoring pollutants in water. *TrAC Trends in Analytical Chemistry* 24, 845–868. <https://doi.org/10.1016/j.trac.2005.06.006>
 48. Wang, P., Yu, J., Zhang, Y., Liu, C., 2013. Groundwater recharge and hydrogeochemical evolution in the Ejina Basin, northwest China. *Journal of Hydrology* 476, 72–86. <https://doi.org/10.1016/j.jhydrol.2012.10.049>
 49. Wang, W., Wang, Zhan, Hou, R., Guan, L., Dang, Y., Zhang, Z., Wang, H., Duan, L., Wang, Zhoufeng, 2018. Modes, hydrodynamic processes and ecological impacts exerted by river–groundwater transformation in Junggar Basin, China. *Hydrogeol J* 26, 1547–1557. <https://doi.org/10.1007/s10040-018-1784-4>
 50. Wałęga, A., Kowalik, T., Bogdał, A., 2016. Estimating the Occurrence of Trends in Selected Elements of a Small Sub-Mountain Catchment Hydrological Regime. *Polish Journal of Environmental Studies*, 25 (5), 2151–2159. <https://doi.org/10.15244/pjoes/62960>
 51. Woessner, W.W., 2000. Stream and Fluvial Plain Ground Water Interactions: Rescaling Hydrogeologic Thought. *Ground Water* 38, 423–429. <https://doi.org/10.1111/j.1745-6584.2000.tb00228.x>
 52. Woessner, W.W., Sullivan, K.E., 1984. Results of Seepage Meter and Mini-Piezometer study, Lake Mead, Nevada. *Ground Water* 22, 561–568. <https://doi.org/10.1111/j.1745-6584.1984.tb01425.x>
 53. Wojak, S., Strużyński, A., Wyrębek, M., 2023. Analysis of changes in hydraulic parameters in a lowland river using numerical modeling. *ASP.FC* 22, 3–17. <https://doi.org/10.15576/ASP.FC/2023.22.1.3>
 54. Xu, W., Su, X., Dai, Z., Yang, F., Zhu, P., Huang, Y., 2017. Multi-tracer investigation of river and groundwater interactions: a case study in Nalenggele River basin, northwest China. *Hydrogeol J* 25, 2015–2029. <https://doi.org/10.1007/s10040-017-1606-0>
 55. Zhu, M., Wang, S., Kong, X., Zheng, W., Feng, W., Zhang, X., Yuan, R., Song, X., Sprenger, M., 2019. Interaction of Surface Water and Groundwater Influenced by Groundwater Over-Extraction, Waste Water Discharge and Water Transfer in Xiong'an New Area, China. *Water* 11, 539. <https://doi.org/10.3390/w11030539>
 56. Żelazo J., 1993. Współczesne poglądy na regulację małych rzek nizinnych: Ochrona przyrody i środowiska w dolinach nizinnych rzek Polski [The recent views on the small lowland river training. In: *Nature and environment conservation in the lowland river valleys in Poland*]. Ed. L. Tomiałojć. Kraków. IOPPAN, 45–154.